

Broadband Dual-frequency High Isolation Base Station Antenna with Low RCS Structure Loaded

Pei-Pei Ma¹, Fang-Fang Fan¹, and Xin-yi Zhao²

¹The Key Laboratory of Antennas and Microwave Technology
Xidian University, Xian, 710071, China
3305559651@qq.com, fffan@mail.xidian.edu.cn

²School of Economics and Management
Beijing University of Posts and Telecommunications, Beijing, 100876, China
3346334629@qq.com

Abstract – A novel dual-band dual-polarization shared aperture antenna is proposed, which covers frequencies 1.7-2.6 GHz and 3.3-3.8 GHz. The structure, with low radar cross section (RCS), is designed to reduce the radiation interference on the high band (HB) antenna. Additionally, by introducing U-shaped slots on the arms of the low band (LB) antenna, polarization isolation between the HB elements is significantly enhanced, which can reach up to 25 dB across the whole band. Moreover, to restore the radiation pattern of the LB antenna, the dielectric substrate is employed beneath the HB antenna as a substitute for the ground plane. The antenna proposed in this paper possesses attributes of broadband, compact size, and simplified structure.

Index Terms – Base station antenna, decoupling, dual band, pattern restoration.

I. INTRODUCTION

With the rapid updating of wireless communication, not only has the number of the wireless users grown exponentially, but also the application scenarios of wireless communication are becoming diverse. Base station antennas, which play a crucial role in the wireless industry infrastructure, have undergone a complex development process. At the junction of 4G and 5G mobile communication, the stage that the 4G and 5G base station antenna will coexist for some time has already arrived.

In the context of limited spatial volume in base stations, three common schemes have been proposed: embedded, stacked, and interleaved structures, as depicted in Fig. 1. The embedded structure allows the high band (HB) antenna to be nested at the center of the low band (LB) antenna. However, this configuration is limited to cases where the frequency of HB is almost twice as large as that of LB [1][2]. The stacked structure involves placing the HB antenna on top of the LB

antenna with a frequency selective surface (FSS) inserted between them to reduce mutual coupling [3–5]. However, this way often leads to complex feed networks and assembly challenges. In contrast, the interleaved structure positions the

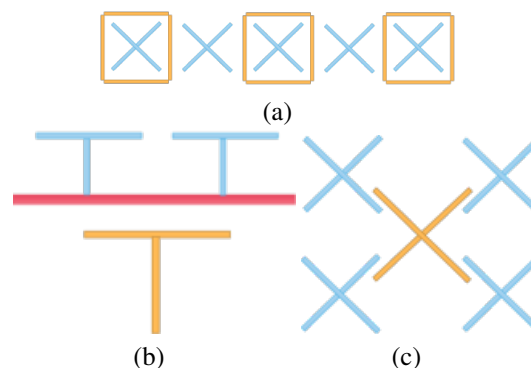


Fig. 1. Structure of the dual-band antenna: (a) embedded structure, (b) stacked structure, and (c) interleaved structure (blue line: the high band element, yellow line: the low band element, red line: FSS).

LB antenna at the center of the HB array, offering advantages in terms of easy installation and manufacturing compared to the other two structures. Moreover, this structure is suitable for any combination of different frequency bands. Therefore, the interleaved structure is adopted in this article. However, the corresponding problems, such as pattern distortion and low isolation, need to be resolved because of the interaction of dual-band antennas.

In order to restore the HB pattern, several significant adjustments to LB radiators have been examined in previous studies. Chokes, as proposed in [6][7], and L-shaped strips introduced in [8], are designed to minimize the induced currents on the LB radiator. Different

types of slots [9][10] and 3-D chokes [11] are adopted to provide induced currents with opposite directions, which helps weaken the scattering influence. Split ring resonators [12] and protruded stubs [13] are used to reduce the radar cross section (RCS) of the LB radiators. At the same time, in [14][15], common-mode (CM) currents induced on the HB antenna generate new resonance interference that worsens the radiation pattern of the LB antenna. To eliminate this CM interference, ferrite-loaded HB coaxial lines and capacitance-loaded HB elements are proposed to restore the LB radiation pattern. Moreover, polarization isolation between the HB elements is another unresolved issue. Additional structures, such as metal walls or parasitic structures [16][17], have been designed to enhance isolation.

In this paper, a novel dual-band dual-polarized base station antenna with compact structure and excellent performance is proposed, which covers broadband of 1.7-2.6 GHz (42%) and 3.3-3.8 GHz (14%). The experimental simulation is carried out based on the ANSYS HFSS. The decoupling approach proposed in this paper is both effective and simple compared to the antenna of similar type. The following is the detailed introduction and analysis.

II. DECOUPLING OF THE DUAL-BAND ANTENNA

The structure of the dual-band shared aperture antenna proposed in this article is shown in Fig. 2. The HB and LB antennas are fed by coaxial lines. The radiation patch and feeding probe are etched on the upper and lower layer of the substrate, respectively, and they are connected to the outer and inner conductor of the coaxial line. To avoid overlap, one of the probes is disconnected in the middle as shown in Figs. 2 (e) and (f).

Figure 3 illustrates the electromagnetic (EM) interference between the HB and LB antenna in the dual-band environment. The radiation of both the HB antenna and LB antenna are adversely affected due to their close proximity and mutual obstruction. The red arrows indicate the transmission of the HB EM wave while the green arrows represent that of the LB EM waves.

A. HB radiation pattern restoration

RCS serves as a critical metric for evaluating the scattering characteristics of targets within radar systems. It quantifies the ratio of the power scattered by a target in the receiving direction to the incident power of plane wave impinging upon the target from a given direction. Currently, extensive research has been devoted to the investigation of low RCS meta-surface, with numerous studies validating their effectiveness. This technological advancement has found practical applications in the design of shared aperture base station antennas, resulting in prominent effects in achieving electromagnetic trans-

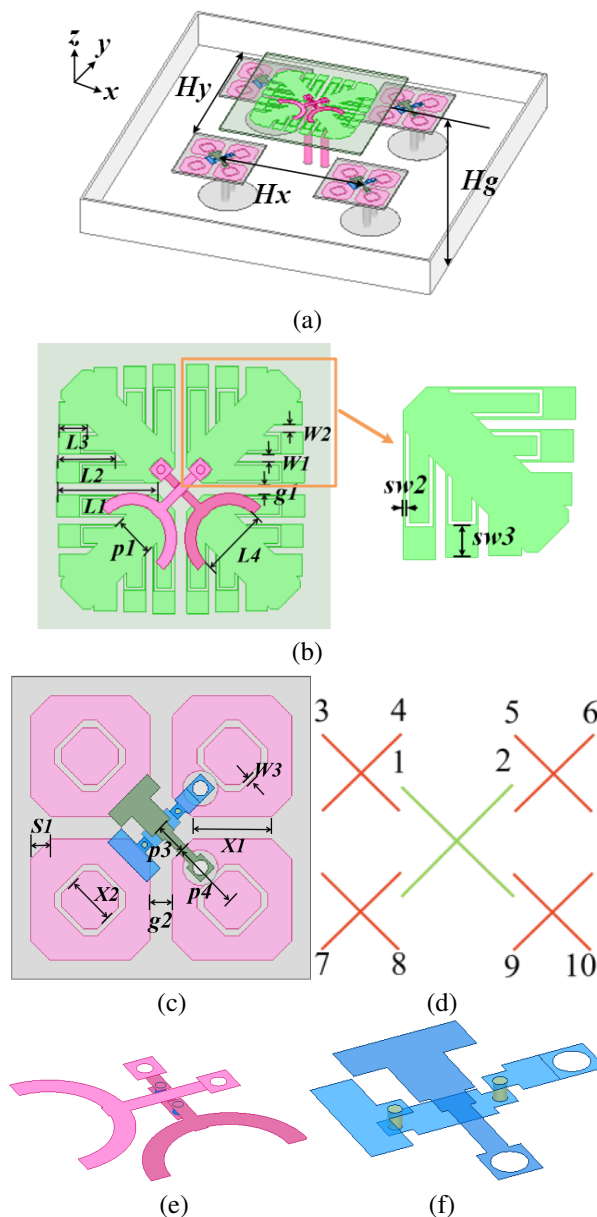


Fig. 2. (a) Overall configuration of the proposed antenna, (b) radiation patch of LB antenna, (c) radiation patch of HB antenna, (d) port distribution, (e) LB feeding probe, and (f) HB feeding probe ($Hx=60$ mm, $Hy=60$ mm, $Hg=30$ mm, $L1=18$ mm, $L2=10.5$ mm, $L3=5$ mm, $L4=12$ mm, $p1=7.32$ mm, $W1=1.23$ mm, $W2=1.3$ mm, $W3=2$ mm, $X1=8$ mm, $X2=5$ mm, $p3=3.1$ mm, $p4=7.07$ mm, $g2=2.25$ mm, $s1=2$ mm, $sw2=0.13$ mm, $sw3=4$ mm).

parency [18][19].

In this paper, a new low RCS structure is designed in this shared aperture base station antenna. Compared to the conventional element with the square patch as the radiator, the antenna element in this design adopts the

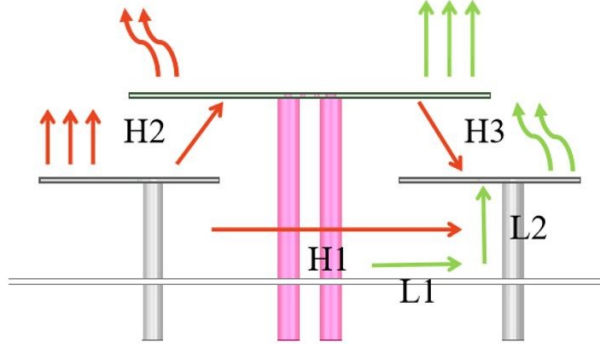


Fig. 3. Transmission path of the EM wave which results in mutual coupling.

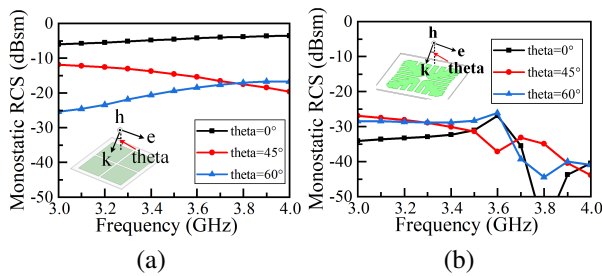


Fig. 4. Comparison of the monostatic RCS between two types of patches under illumination of plane waves at different incident angles: (a) square-shaped patch and (b) branch-shaped patch.

branch-shaped structure. This design greatly improves the scattering interference on the HB antenna due to the low RCS property of the LB antenna element itself. Figure 4 illustrates the monostatic RCS value of the different radiation patches. As the incident angle of the plane wave varies, the RCS of the square patch remains above -25 dB, reaching up to -5 dB under normal incidence. In contrast, the RCS of the proposed branch-shaped patch remains below -25 dB across the entire frequency band. Figure 5 illustrates the comparison of the electric field in the horizontal plane when the HB antenna is excited. It can be observed that the conventional LB element with square patch causes strong interference with the radiation of the HB antenna. However, the proposed antenna exhibits a nearly restored electric field distribution similar to its original state. Therefore, the radiation pattern of HB antenna exhibits significant improvement, as shown in Fig. 6. The issues of distortion and deflection of the HB pattern is effectively resolved.

B. In-band decoupling of HB elements

In the environment of dual-band antenna, the polarization isolation between the HB elements is influenced by the LB antenna as well. The positioning of the LB antenna introduces additional coupling path between

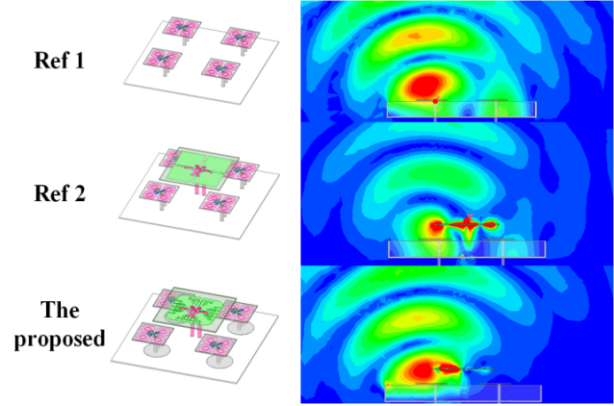


Fig. 5. Comparison of E-field distribution at xoz plane when port 3 is excited at 3.5 GHz.

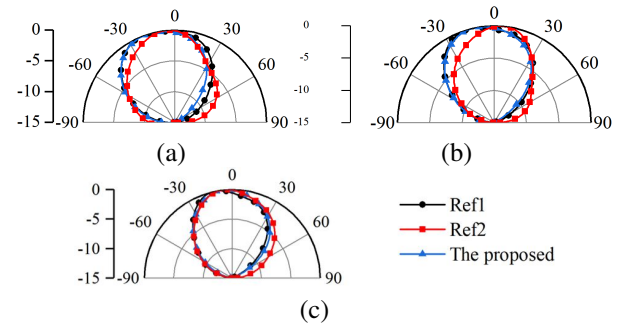


Fig. 6. Comparison of HB normalized radiation pattern in xoz plane when port 3 is excited: (a) 3.3 GHz, (b) 3.55 GHz, and (c) 3.8 GHz.

the HB antenna elements, as depicted in Fig. 3, which adversely impacts the isolation. The H3 represents the reflected coupled wave caused by the LB antenna and the H1 represents the direct coupled wave between the HB elements. To mitigate this effect, a beneficial approach is to add a parasitic structure or adjust the parameters of the LB radiator which affect the isolation. These structural adjustments induce change in the amplitude and phase of the reflected coupled wave (H3). If the amplitude of H3 and H1 are the same but the phase difference is 180° , their effects can cancel each other out. The challenge is to improve the isolation without compromising the low scattering performance of LB antenna.

In this paper, the U-shaped slots are employed on the arms of the LB antenna, which has proven to be effective, as shown in Fig. 7. Therefore, by appropriately adjusting the dimensions of the U-shaped slots, the isolation of HB elements is maintained above 25 dB across the entire band.

C. LB radiation pattern restoration

When the LB antenna is excited, as shown in Fig. 8, the current flows along the ground plane towards the

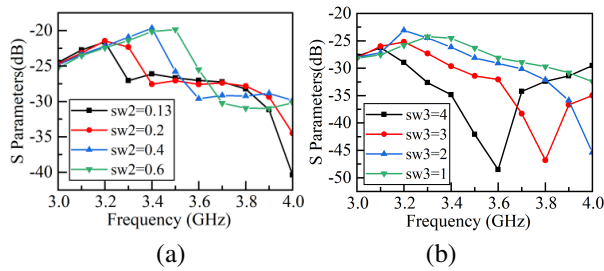


Fig. 7. The influence of U-shaped slots on the isolation between HB elements (a) S63 and (b) S53.

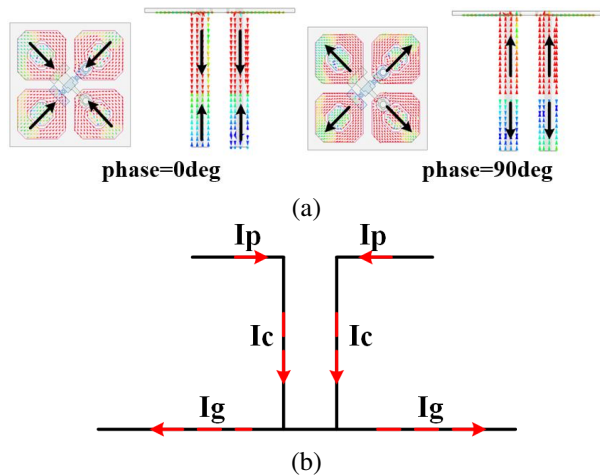


Fig. 8. (a) Current distribution on HB element at different phase when LB is excited, and (b) current distribution model of HB antenna.

HB antenna (I_g), subsequently reaching radiation patch of the HB element (I_c and I_p). The HB antenna can be viewed as a monopole antenna with a metal patch loaded on its top, which precisely resonates at the LB band, thereby causing the degradation of LB radiation pattern. Therefore, to prevent the coupling current along the ground, the substrate is employed beneath the HB antenna instead of the ground plane.

As shown in Fig. 9, prior to the adjustment, when the

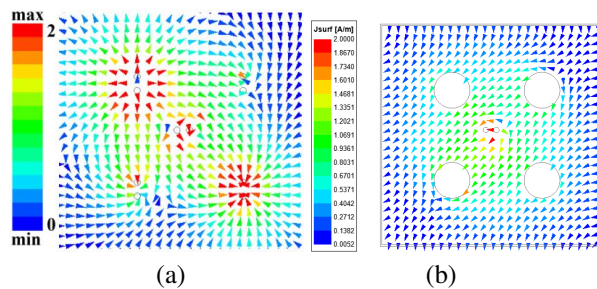


Fig. 9. Current distribution on the ground when LB is excited: (a) unmodified ground and (b) modified ground.

LB antenna is excited, there are strong currents flowing along the ground into the coaxial of the HB antenna. Correspondingly, there is a noticeable alteration in the current flow direction on the ground plane after the adjustment. The comparison of the electric field plots in Fig. 10 demonstrates the effect of the ground plane adjustment. At 1.7 GHz, the interference caused by HB antenna leads to cancellation of the electric field, resulting in the near-zero gain value. However, after the modification, the disrupted current flow on the ground effectively eliminates the influence of the HB antenna on the LB antenna.

The results of the radiation pattern of the proposed LB antenna compared with that of the antenna without decoupling are shown in Fig. 11, indicating that the problems mentioned above have been resolved.

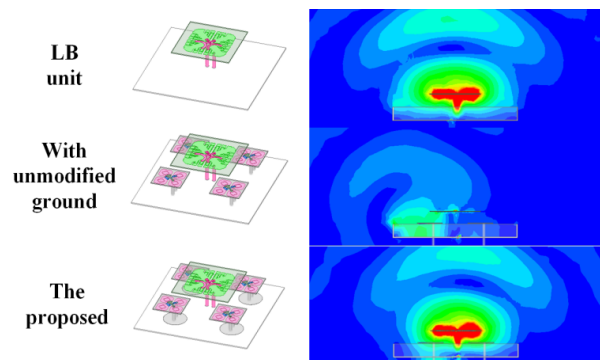


Fig. 10. Comparison of E-field distribution at xoz plane when port 1 is excited at 1.7 GHz.

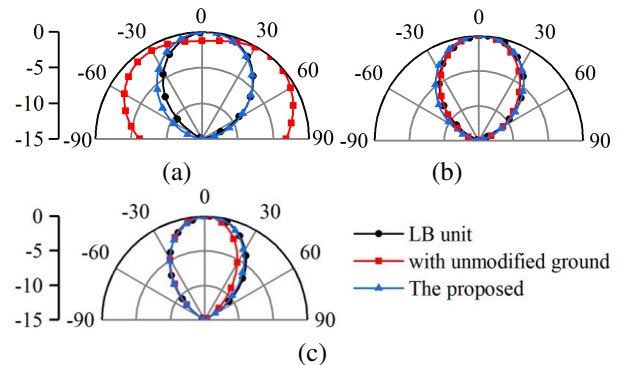


Fig. 11. Comparison of LB radiation pattern in xoz plane when port 1 is excited: (a) 1.7 GHz, (b) 2.2 GHz, and (c) 2.6 GHz.

III. RESULTS AND DISCUSSION

The antenna is fabricated and measured as shown in Fig. 12. The simulated and measured results of the proposed antenna are presented as follows. Due to the symmetric characteristics of the antenna, the results of partial ports are provided. Figure 13 showcases the S-parameters of the HB antenna, with the VSWR less than

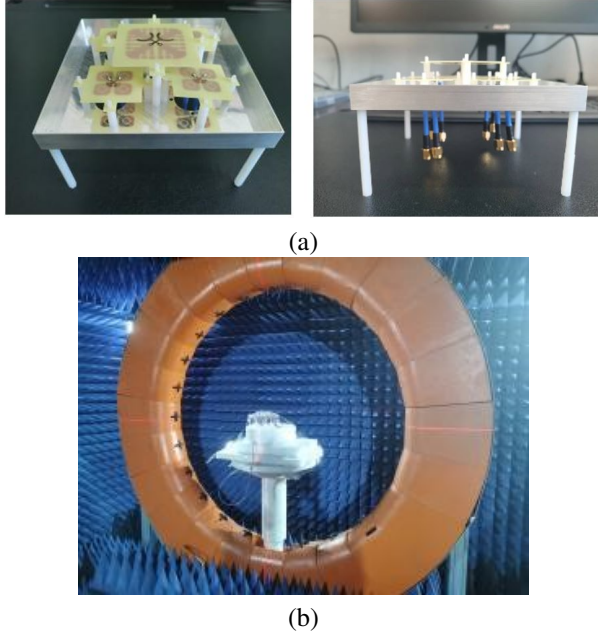


Fig. 12. (a) Fabricated antenna model and (b) measure environment for the antenna.

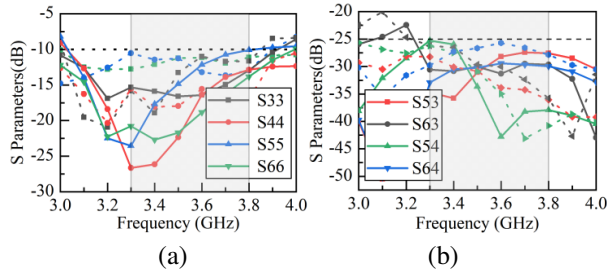


Fig. 13. Simulated and measured S-parameters for HB antenna. (a) Reflection coefficient of HB ports, and (b) polarization isolation between the adjacent HB antenna elements (solid line: simulated, dash line: measured).

2 and polarization isolation greater than 25 dB from 3.3-3.8 GHz. Similarly, Fig. 14 exhibits the S-parameters of the LB antenna, with the VSWR less than 1.5 from 1.7-2.6 GHz. The simulated and measured S-parameter results demonstrate excellent agreement.

The simulated and measured gain ranges from 6.7 dBi to 8.2 dBi and 6.5 dBi to 8.6 dBi for the HB antenna, and from 6.4 dBi to 8.3 dBi and 6 dBi to 8.1 dBi for the LB antenna, as shown in

Figure 15 The measured gain of the LB antenna is slightly lower than the simulated results. While parts of the measured gain for the HB antenna are slightly higher than the simulated results. Figures 16 (a) and (b) illustrate the simulated and measured radiation patterns of LB and HB antenna when the +45° port is excited.

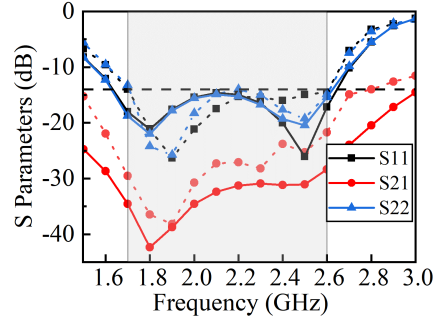


Fig. 14. Simulated and measured S-parameters for LB antenna (solid line: simulated, dash line: measured).

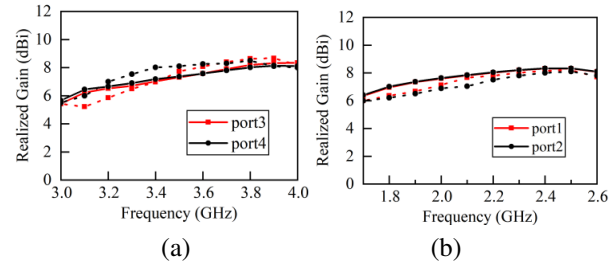


Fig. 15. Simulated and measured gain. (a) HB antenna and (b) LB antenna (solid line: simulated, dash line: measured).

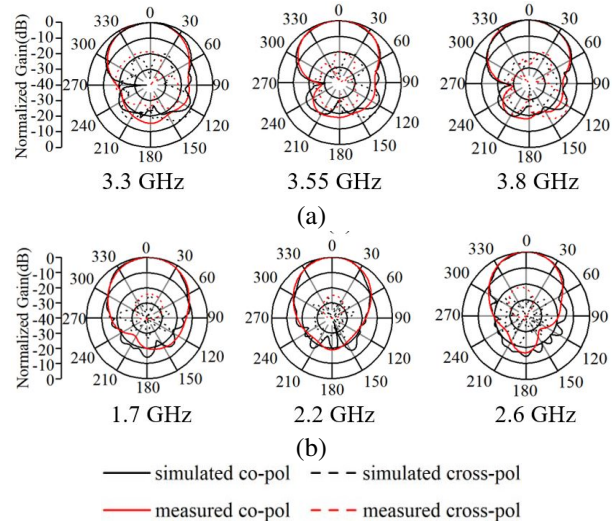







Fig. 16. Simulated and measured radiation pattern for HB and LB antenna at xoz plane when (a) port 3 and (b) port 1 is excited.

The discrepancies between the simulated and measured results are due to manufacturing and measurement errors.

Table 1 shows the comparison of the proposed dual-band base station antenna with previous antennas from

Table 1: Comparison with the antenna from previous article

| | Bandwidth (GHz) | Hg | HB Isolation | Overall Structure |
|-----------|----------------------|-----------------|--------------|---|
| [16] | 1.71-2.17 3.3-3.8 | $0.28\lambda_L$ | >20 dB |  |
| [6] | 1.71-2.26 3.3-3.7 | N | >25 dB |  |
| [5] | 1.7-2.4 3.3-3.8 | $0.50\lambda_L$ | N |  |
| [17] | 1.7-2.2 3.3-3.6 | $0.25\lambda_L$ | >20 dB |  |
| This work | 1.7-2.6 3.3-3.8 | $0.21\lambda_L$ | >25 dB |  |

KEY: λ_L center frequency of LB, N not given
Hg overall profile height

other research articles. Firstly, the proposed antenna has a significantly wider bandwidth and a simpler structure for achieving dual-band decoupling. Extra structure to realize the mutual coupling suppression is not needed in this paper, such as meta-surface utilized in [5][16] or parasitic structure and metal walls applied in [17]. Secondly, the antenna has a lower profile height compared to the antenna designed in [5][16][17]. Lastly, the isolation between the HB elements of the proposed antenna is superior to that of the antenna proposed in [16][17]. In summary, the antenna proposed in this paper offers advantages of broadband, miniaturization, and high isolation. It provides a practical solution for dual-band base station antennas, addressing the limitations of previous designs.

IV. CONCLUSION

This article proposes an effective decoupling method for the dual-band antenna. The low RCS structure as LB radiator is designed to eliminate the scattering interference on HB antenna. The modified ground beneath the HB antenna is introduced to mitigate the CM interference of the HB antenna on the LB element. Moreover, the U-slots loaded on the LB arms significantly enhance isolation between the HB elements by altering the magnitude and phase of the reflected wave. The experimental results presented validate the effectiveness of the proposed decoupling method. In short, the dual-band antenna developed in this study is highly suitable for base station antenna applications.

REFERENCES

- [1] H. Huang, Y. Liu, and S. Gong, "A novel dual-broadband and dual-polarized antenna for 2G/3G/LTE base stations," *IEEE Transactions on Antennas and Propagation*, vol. 64, no. 9, pp. 4113-4118, Sep. 2016.
- [2] F. Jia, S. Liao, and Q. Xue, "A dual-band dual-polarized antenna array arrangement and its application for base station antennas," *IEEE Antennas and Wireless Propagation Letters*, vol. 19, no. 6, pp. 972-976, June 2020.
- [3] D. He, Y. Chen, and S. Yang, "A low-profile triple-band shared-aperture antenna array for 5g base station applications," *IEEE Transactions on Antennas and Propagation*, vol. 70, no. 4, pp. 2732-2739, Apr. 2022.
- [4] Y. Zhu, Y. Chen, and S. Yang, "Decoupling and low-profile design of dual-band dual-polarized base station antennas using frequency-selective surface," *IEEE Transactions on Antennas and Propagation*, vol. 67, no. 8, pp. 5272-5281, Aug. 2019.
- [5] Y. Zhu, Y. Chen, and S. Yang, "Cross-band mutual coupling reduction in dual-band base-station antennas with a novel grid frequency selective surface," *IEEE Transactions on Antennas and Propagation*, vol. 69, no. 12, pp. 8991-8996, Dec. 2021.
- [6] H.-H. Sun, H. Zhu, C. Ding, B. Jones, and Y. J. Guo, "Scattering suppression in a 4G and 5G base station antenna array using spiral chokes," *IEEE Antennas and Wireless Propagation Letters*, vol. 19, no. 10, pp. 1818-1822, Oct. 2020.
- [7] H.-H. Sun, C. Ding, H. Zhu, B. Jones, and Y. J. Guo, "Suppression of cross-band scattering in multiband antenna arrays," *IEEE Transactions on Antennas and Propagation*, vol. 67, no. 4, pp. 2379-2389, Apr. 2019.
- [8] Z. Chen, T. Xu, J.-F. Li, L. H. Ye, and D.-L. Wu, "Dual-broadband dual-polarized base station antenna array with stable radiation pattern," *IEEE Antennas and Wireless Propagation Letters*, vol. 22, no. 2, pp. 303-307, Feb. 2023.
- [9] Y.-S. Wu, Q.-X. Chu, and H.-Y. Huang, "Electromagnetic transparent antenna with slot-loaded patch dipoles in dual-band array," *IEEE Transactions on Antennas and Propagation*, vol. 70, no. 9, pp. 7989-7998, Sep. 2022.
- [10] Q.-X. Chu, Y.-S. Wu, and Y.-L. Chang, "A novel electromagnetic transparent antenna in dual-band shared-aperture array," *IEEE Transactions on Antennas and Propagation*, vol. 70, no. 10, pp. 9894-9899, Oct. 2022.
- [11] J. Jiang and Q.-X. Chu, "Dual-band shared-aperture base station antenna array based on 3-D

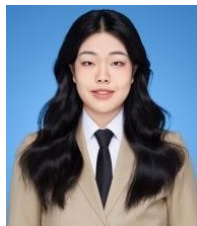
- chokes,” *IEEE Antennas and Wireless Propagation Letters*, vol. 22, no. 4, pp. 824-828, Apr. 2023.
- [12] Y.-L. Chang and Q.-X. Chu, “Broadband dual-polarized electromagnetic transparent antenna for cross-band scattering suppression,” *IEEE Antennas and Wireless Propagation Letters*, vol. 21, no. 7, pp. 1452-1456, July 2022.
- [13] Y. Li and Q.-X. Chu, “Dual-band base station antenna array using the low-band antenna as parasitic decoupler,” *IEEE Antennas and Wireless Propagation Letters*, vol. 21, no. 7, pp. 1308-1312, July 2022.
- [14] H.-H. Sun, B. Jones, Y. J. Guo, and Y. H. Lee, “Suppression of cross-band scattering in interleaved dual-band cellular base-station antenna arrays,” *IEEE Access*, vol. 8, pp. 222486-222495, 2020.
- [15] Y.-L. Chang and Q.-X. Chu, “Ferrite-loaded dual-polarized antenna for decoupling of multiband multiarray antennas,” *IEEE Transactions on Antennas and Propagation*, vol. 69, no. 11, pp. 7419-7426, Nov. 2021.
- [16] S. J. Yang, R. Ma, and X. Y. Zhang, “Self-decoupled dual-band dual-polarized aperture-shared antenna array,” *IEEE Transactions on Antennas and Propagation*, vol. 70, no. 6, pp. 4890-4895, June 2022.
- [17] Y. Li and Q.-X. Chu, “Self-decoupled dual-band shared-aperture base station antenna array,” *IEEE Transactions on Antennas and Propagation*, vol. 70, no. 7, pp. 6024-6029, July 2022.
- [18] G. Su, W. Che, W. Yang, Q. Xue, B.-L. Bu, P. Liu, and L. Chen, “Low-scattering dipole antenna using mushroom-shaped structure for applications in dual-band shared-aperture array,” *IEEE Antennas and Wireless Propagation Letters*, vol. 22, no. 1, pp. 159-163, Jan. 2023.
- [19] S. J. Yang, Y. Yang, and X. Y. Zhang, “Low scattering element-based aperture-shared array for multi-band base stations,” *IEEE Transactions on Antennas and Propagation*, vol. 69, no. 12, pp. 8315-8324, Dec. 2021.



Pei-Pei Ma received her bachelor's degree from Hainan University in July 2019 and she is currently pursuing the master's degree at Xidian University from September 2021. Her research interests mainly concentrated on the base station antennas and filters.



Fang-Fang Fan received a Ph.D. degree in Electromagnetic Field and Microwave Technology from Xidian University in 2011. Currently, she is an associate professor at Xidian University. Her current research interests include antenna arrays, gap waveguide technology, and base station antennas for 5G application.



Xin-yi Zhao is currently pursuing the bachelor's degree of Intelligence and Innovation Management at Beijing University of Posts and Communications from September 2022. Her research interests include data analysis and digital economy.